

# Light energy storage in TiO<sub>2</sub>/MnO<sub>2</sub> composite electrode for photoelectrochemical capacitor

*Hiroyuki Usui<sup>\*,†,§</sup>, Kentaro Koseki<sup>†,§</sup>, Takahiro Tamura<sup>†,§</sup>, Yasuhiro Domi<sup>†,§</sup>, and Hiroki Sakaguchi<sup>†,§</sup>*

<sup>†</sup> Department of Chemistry and Biotechnology, Graduate School of Engineering, Tottori University, 4-101 Minami, Koyama-cho, Tottori 680-8552, Japan

<sup>§</sup> Center for Research on Green Sustainable Chemistry, Tottori University, 4-101 Minami, Koyama-cho, Tottori 680-8552, Japan

Corresponding Author: \* Tel./Fax: +81-857-31-5634, E-mail: usui@chem.tottori-u.ac.jp

## **Abstract**

Composite electrodes comprising TiO<sub>2</sub> and MnO<sub>2</sub> particles were prepared as photoelectrochemical capacitor electrodes that enable both photoelectric conversion and energy storage. A MnO<sub>2</sub> electrode was also prepared for characterization of MnO<sub>2</sub> alone, and its electrochemical capacitor property was evaluated. The MnO<sub>2</sub> electrode showed higher specific capacitance than a RuO<sub>2</sub> electrode. Results of the photoelectrochemical measurements demonstrated that the discharge capacity of the TiO<sub>2</sub>/MnO<sub>2</sub> composite electrode was slightly inferior to that of the TiO<sub>2</sub> and RuO<sub>2</sub> electrodes using. By reducing MnO<sub>2</sub> particle size, the composite electrode exhibited increased surface roughness and enhanced capacity. We consider that the smaller MnO<sub>2</sub> particles can efficiently store Na<sup>+</sup> ions even at a low photo-charge voltage of TiO<sub>2</sub>.

**Keywords:** Photoelectrochemical capacitor; Composite electrode; Rutile-type titanium oxide; Manganese oxide

## 1. Introduction

In realizing a low-carbon society, promotion of renewable energy, particularly solar energy, will play a crucial role. However, a disadvantage of solar energy is that solar irradiance strongly varies depending on weather, time of day, and location, resulting in unstable power generation and a demand for energy storage. Electricity generated by a photovoltaic cell is generally stored using a Li-ion battery or an electrochemical capacitor connected to the cell via an external circuit. Another disadvantage is the low power density ( $1.36 \text{ kW m}^{-2}$ ) of solar irradiance. Thus, solar power is unfavorable for current portable electronic devices with high power demands; however, it will be sufficiently useful for next-generation display devices like electronic paper, which have much lower power consumption. To increase storage efficiency and decrease device size, a single electrode should achieve both photoelectric conversion and energy storage, as some researchers have reported [1-3].

Titanium dioxide ( $\text{TiO}_2$ ) is a popular photo-semiconductor with excellent chemical stability in aqueous solution. Photoexcited electrons are generated by irradiation of the  $\text{TiO}_2$  electrode, which reduce other transition metal oxides; thus  $\text{TiO}_2$  electrodes can act as energy-storage electrodes. Joudkazytè *et al.* have recently developed a photoelectrochemical capacitor consisting of two electrodes: a  $\text{TiO}_2$  electrode for power generation and a  $\text{RuO}_2$  electrode for energy storage in aqueous solution [4]. Tatsuma *et al.* have reported a photoelectrochemical capacitor comprising a  $\text{TiO}_2$  electrode and a  $\text{WO}_3$  electrode [5], used for power generation and energy storage, respectively. The material costs of  $\text{RuO}_2$  and  $\text{WO}_3$  are higher than the cost of  $\text{TiO}_2$ . In this study, we chose  $\text{MnO}_2$  as the energy storage material because of its lower cost, and a novel single electrode comprising a  $\text{TiO}_2/\text{MnO}_2$  composite was prepared as a photoelectrochemical capacitor.

## 2. Materials and Methods

### 2.1. Active materials of electrodes

As-received manganese dioxide powder ( $\epsilon\text{-MnO}_2$ , Akhtenskite, Wako Pure Chemical Industries) was used as the active material. The  $\text{MnO}_2$  powder has an average particle size of

11.8  $\mu\text{m}$  and crystallite size of 11.6 nm (Fig. S1 and Fig. S2 in Supporting Information). To reduce the particle size of  $\text{MnO}_2$ , a mechanical milling treatment was conducted by a high-energy planetary ball mill (P-6, Fritsch) for 1 h with a rotational speed of 380 rpm. For the photo-semiconductor, we used titanium dioxide powder (rutile  $\text{TiO}_2$ , Wako Pure Chemical Industries) with a particle size of 213 nm and crystallite size of 41.1 nm. Thick-film electrodes of  $\text{TiO}_2/\text{MnO}_2$  composite were prepared by the gas-deposition (GD) method [6,7]. The detailed procedures are described in Fig. S3.

## 2.2. Charge–discharge tests as electrochemical capacitor

Conventional charge–discharge tests were conducted in a beaker-type three-electrode cell (HX-113, Hokuto Denko Co., Ltd.). A titanium wire and a  $\text{Ag}/\text{AgCl}$  electrode were used as the counter and reference electrodes, respectively. The electrolyte was a  $\text{Na}_2\text{SO}_4$  aqueous solution with a concentration of  $0.5 \text{ mol L}^{-1}$ . Galvanostatic charge–discharge method was applied using a battery test system (HJ-1001 SM8A, Hokuto Denko Co., Ltd.) with a potential range of 0.04–0.84 V under  $200 \text{ mA g}^{-1}$  at 303 K. By a linear approximation for the charge–discharge curves, the specific capacitance  $C_s$  was calculated using the capacitance calculator software (SD8 CAR, Hokuto Denko Co., Ltd.) and the following equation:

$$C_s = I / [(dV/dt) m]$$

where  $I$  is the charge–discharge current,  $dV/dt$  is the scan rate, and  $m$  is the active material mass.

## 2.3. Photoelectrochemical measurements

Photoelectrochemical measurements were performed using the same cell as the electrochemical capacitor test. Our newly developed measurement system is shown in Fig. 1. As a solar simulator, a Xe lamp (SOLAX XC-100EFSS, SERIC Co., Ltd.) with a power density of about  $1.0 \text{ kW m}^{-2}$  was used. In a photo-charge process, the  $\text{TiO}_2/\text{MnO}_2$  electrode was irradiated for 10 s in open-circuit condition. A discharge process was subsequently performed for 20 s in short-circuit condition between the  $\text{TiO}_2/\text{MnO}_2$  electrode and the Ti electrode. For a control experiment, the discharge current was measured after the electrodes were kept in open-circuit condition for 10 s without irradiation (a dark-charge process). Typical variations in potential and current density are shown in Fig. S5. The discharge capacity was defined as an integrated

difference between the two kinds of discharge currents after the photo-charge dark-charge processes during the first cycles (Fig. S6).

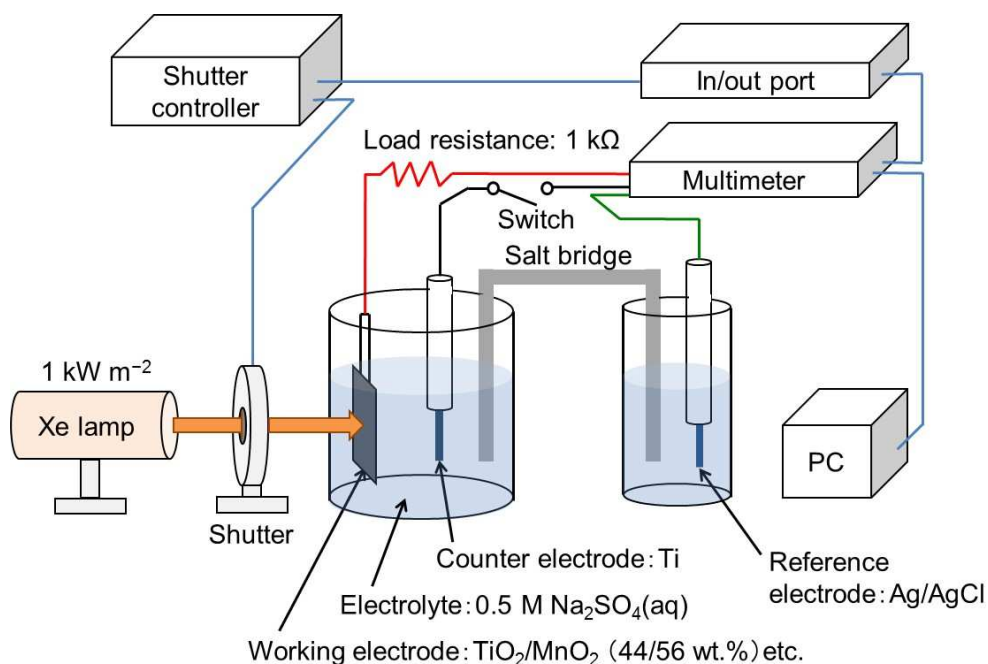


**Figure 1.** Schematic illustration of measurement system for photoelectrochemical capacitor electrode.

### 3. RESULTS AND DISCUSSION

#### 3.1. Electrochemical properties as capacitor electrode.

The charge–discharge curve of the  $\text{RuO}_2$  electrode shows a symmetric profile (Fig. S4(a)), indicating typical pseudo-capacitive characteristics and a reversible redox-based variation of oxidation states among  $\text{Ru}^{4+}$ ,  $\text{Ru}^{3+}$ , and  $\text{Ru}^{2+}$ . On the other hand, the  $\text{MnO}_2$  electrode exhibits a large potential drop at the beginning of the discharge process (Fig. S4(b)), probably due to the large overpotential caused by the much lower electronic conductivity of  $\text{MnO}_2$  ( $10^{-6} \text{ S cm}^{-1}$ ) than  $\text{RuO}_2$  ( $10^4 \text{ S cm}^{-1}$ ), which indicates that the electrode reaction is limited to the surface of the  $\text{MnO}_2$  electrode. The pseudo-capacitance of  $\text{MnO}_2$  arises from the  $\text{Mn}^{4+}/\text{Mn}^{3+}$  redox reaction at the surface of  $\text{MnO}_2$  particles [8].  $\epsilon$ - $\text{MnO}_2$  has one-dimensional tunnel structures of  $1 \times 1$  and

1×2, corresponding to sizes of 0.23 nm × 0.23 nm and 0.23 nm × 0.46 nm, respectively [9]. To retain charge balance of reduced MnO<sub>2</sub>, Na<sup>+</sup> ions of the electrolyte are inserted into the tunnel structures on the MnO<sub>2</sub> surface because the ionic diameter of a Na<sup>+</sup> ion (0.204 nm) is smaller than either tunnel size.

Figure 2 shows the specific capacitance variation for the MnO<sub>2</sub> electrode versus cycle number. The capacitances for the RuO<sub>2</sub> and TiO<sub>2</sub> electrodes were plotted for comparison. The capacitance of the TiO<sub>2</sub> electrode was almost 0 F g<sup>-1</sup>, suggesting that no electrochemical redox reaction occurs in the potential range of 0.0–0.8 V vs. Ag/AgCl. We have previously reported that Na-insertion into rutile TiO<sub>2</sub> can occur in the potential range of 0.1–0.7 V vs. Na<sup>+</sup>/Na [10], which corresponds to the potential range of –2.4 to –1.8 V vs. Ag/AgCl. The RuO<sub>2</sub> electrode maintained a constant capacitance of 320–330 F g<sup>-1</sup>, which is smaller than the typical capacitances of 500–600 F g<sup>-1</sup> [11]. This is attributed to the preparation method in this study: the electrodes do not include any binder or conductive additive for the fundamental evaluation. The MnO<sub>2</sub> electrode exhibited a larger capacitance of 276 F g<sup>-1</sup> in the first cycle, although rapid capacitance decay was observed for the initial ten cycles. The capacitance decay presumably arises from an irreversible change in the MnO<sub>2</sub> crystal structure.

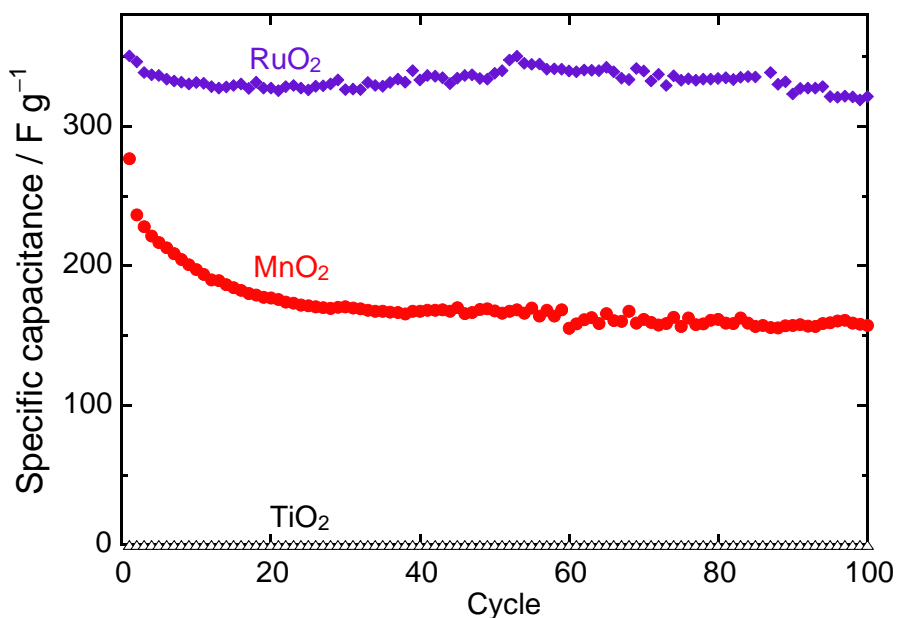


**Figure 2.** Dependence of specific capacitance on cycle number for MnO<sub>2</sub> electrode as electrochemical capacitor. For comparison, we prepared RuO<sub>2</sub> electrode and TiO<sub>2</sub> electrode, and evaluated their specific capacitances.

### 3.2. Charge–discharge properties as photoelectrochemical capacitor.

Figure 3(a) represents the discharge capacity of the composite electrode prepared using TiO<sub>2</sub> and as-received MnO<sub>2</sub>. In this study, a TiO<sub>2</sub>/RuO<sub>2</sub> composite electrode was also prepared and evaluated for comparison. The discharge capacity of this composite electrode (Fig. S7) was inferior to that obtained by other researchers for a photoelectrochemical capacitor comprised of individual TiO<sub>2</sub> and RuO<sub>2</sub> electrodes [4]. Thus, Fig. S7 shows the value of their work as a standard. The TiO<sub>2</sub> electrode delivered a capacity of only 8.7 mA h g<sup>-1</sup>. Compared to this, the TiO<sub>2</sub>/MnO<sub>2</sub> composite electrode presented a higher capacity of 30 mA h g<sup>-1</sup>. However, this capacity is slightly inferior to the TiO<sub>2</sub>/RuO<sub>2</sub> composite electrode [4].

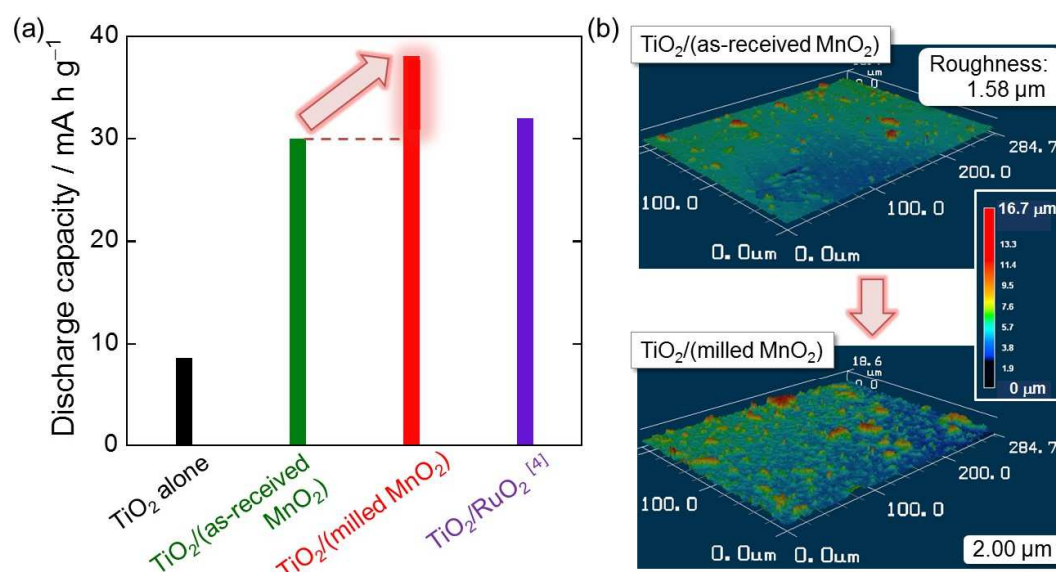


**Figure 3.** (a) Discharge capacities of composite electrodes of TiO<sub>2</sub>/(as-received MnO<sub>2</sub>) and TiO<sub>2</sub>/(milled MnO<sub>2</sub>). (b) Surface morphologies of these electrodes observed by confocal scanning laser microscope. By mechanical milling for MnO<sub>2</sub> powder, root mean square roughness of the composite electrode increased from 1.58 μm to 2.00 μm.

The difference in the capacities obviously originates from the storage/extraction of Na<sup>+</sup> ions into/from MnO<sub>2</sub> induced by the photoelectrochemical reaction, due to an insufficient photo-charge voltage of irradiated TiO<sub>2</sub>, which is observed as a potential drop of approximately 0.3 V

(Fig. S5). Owing to this low photo-charge voltage, Na<sup>+</sup> ions can be stored in only near-surface regions of MnO<sub>2</sub> particles. We mechanically milled the MnO<sub>2</sub> powder to reduce its particle size, thereby enhancing the discharge capacity of the composite electrode. Figure 3(b) compares surface morphologies of the TiO<sub>2</sub>/MnO<sub>2</sub> composite electrodes prepared using the as-received MnO<sub>2</sub> powder and the milled MnO<sub>2</sub> powder. The root-mean-square roughness was increased from 1.58 μm to 2.00 μm by the milling of MnO<sub>2</sub>. As expected, the discharge capacity of the TiO<sub>2</sub>/(milled MnO<sub>2</sub>) electrode exhibited a higher capacity (38 mA h g<sup>-1</sup>) than both the TiO<sub>2</sub>/(as-received MnO<sub>2</sub>) electrode and the TiO<sub>2</sub>/RuO<sub>2</sub> electrode [4]. Thus, we achieved higher capacity using less expensive materials, TiO<sub>2</sub> and MnO<sub>2</sub>, and this performance was attained not in two individual electrodes but in a single composite electrode.

#### 4. Conclusions

We prepared composite electrodes comprising TiO<sub>2</sub> and MnO<sub>2</sub> particles by GD, and investigated their charge–discharge properties for photoelectric conversion and energy storage. The discharge capacity of the TiO<sub>2</sub>/MnO<sub>2</sub> electrode was slightly inferior to that of electrodes composed of TiO<sub>2</sub> and RuO<sub>2</sub>; however, by reducing the size of MnO<sub>2</sub> particles, the capacity of the composite electrode successfully enhanced. We found that the smaller MnO<sub>2</sub> particles can store Na<sup>+</sup> ions more efficiently even at a low photo-charge voltage of TiO<sub>2</sub>.

#### Acknowledgements

This work was partially supported by Japan Society for the Promotion of Science (JSPS) KAKENHI (24350094, 15K21166, 16K05954), and the Matching Planner Program from the Japan Science and Technology Agency (JST) (MP28116808236). A part of this work was supported by the Japan Association for Chemical Innovation (JACI) and the Izumi Science and Technology Foundation. The authors thank the reviewers for their helpful suggestions.

#### References

- [1] H. Usui, O. Miyamoto, T. Nomiya, Y. Horie, T. Miyazaki, *Sol. Energy Mater. Sol. Cells*, **86** (2005) 123–134.
- [2] T. Nomiya, K. Sasabe, K. Sakamoto, Y. Horie, *Jpn. J. Appl. Phys.*, **54** (2015) 071101-1–5.
- [3] T. Chen, L. Qiu, Z. Yang, Z. Cai, J. Ren, H. Li, H. Lin, X. Sun, H. Peng, *Angew. Chem. Int. Ed.*, **51** (2012) 11977–11980.
- [4] J. Juodkazytė B. Šebeka, P. Kalinauskas, K. Juodkazis, *J. Solid State Electrochem.*, **14** (2010) 741–746.

- [5] Y. Takahashi, T. Tatsuma, *Electrochem. Commun.*, **10** (2008) 1404–1407.
- [6] H. Sakaguchi, T. Toda, Y. Nagao, T. Esaka, *Electrochem. Solid-State Lett.*, **10** (2007) J146–J149.
- [7] H. Usui, Y. Kiri, H. Sakaguchi, *Thin Solid Films*, **520** (2012) 7006–7010.
- [8] M. Toupin, T. Brousse, D. Belanger, *Chem. Mater.*, **16** (2004) 3184–3190.
- [9] K. Chen, C. Sun, D. Xue, *Phys. Chem. Chem. Phys.*, **17** (2015) 732–750.
- [10] H. Usui, S. Yoshioka, K. Wasada, M. Shimizu, H. Sakaguchi, *ACS Appl. Mater. Interfaces*, **7** (2015) 6567–6573.
- [11] Y.-F. Ke, D.-S. Tsai, Y.-S. Huang, *J. Mater. Chem.*, **15** (2005) 2122–2127.

### Figure Captions

Figure 1. Schematic illustration of measurement system for photoelectrochemical capacitor electrode.

Figure 2. Dependence of specific capacitance on cycle number for MnO<sub>2</sub> electrode as electrochemical capacitor. For comparison, we prepared RuO<sub>2</sub> electrode and TiO<sub>2</sub> electrode, and evaluated their specific capacitances.

Figure 3. (a) Discharge capacities of composite electrodes of TiO<sub>2</sub>/(as-received MnO<sub>2</sub>) and TiO<sub>2</sub>/(milled MnO<sub>2</sub>). (b) Surface morphologies of these electrodes observed by confocal scanning laser microscope. By mechanical milling for MnO<sub>2</sub> powder, root mean square roughness of the composite electrode increased from 1.58 μm to 2.00 μm.